

Filamentous Artificial Virus from a Self-Assembled Discrete Nanoribbon**

Yong-beom Lim, Eunji Lee, You-Rim Yoon, Myeong Sup Lee, and Myongsoo Lee*

The creation of virus-like nanomaterials (artificial viruses) has been the subject of intensive research in the field of gene/drug delivery because of their huge therapeutic potential.^[1] Some progress has been made in the field; however, compared to the natural viruses, which are evolution-tailored experts in gene delivery, the synthetic system is still far behind the natural system. One of the critical reasons for this shortcoming is that the size and shape of the artificial viruses, among the most important determinants of their efficiency, are very difficult to control.

As the polyanionic nature of nucleic acids (DNA and RNA) prevents them from crossing the same charged cytoplasmic membrane barrier, a vector system is necessary to neutralize their charge and to install other functions, such as cell binding, endosome escape, and nucleus localization. Although there are serious safety concerns, such as immunogenicity and carcinogenesis, in the use of viral vectors, they are still far more widely used for gene therapy than nonviral vectors (artificial viruses) because of their higher efficiency.^[1a]

The basic principle of artificial virus formation is a condensation reaction which is induced by the attraction between oppositely charged molecules (for example, between cationic polymer and DNA).^[2] However, this polyion coupling generally leads to the formation of huge nanoaggregates that are highly heterogeneous in size and shape, and is uncontrollable in most cases.^[3] In regard to the size issue, a certain optimal size exists for the nanoparticulate delivery systems to work best. The shape of the nanoparticle can also be a crucial factor. For example, sometimes the cylindrical (that is, filamentous) nanostructure has certain advantages over the spherical one in that it persists longer in vivo,^[4] which might explain why many filamentous viruses exist in nature. Therefore, it is imperative to find a general strategy to control the size and shape of artificial viruses.

Recent advances in supramolecular chemistry have made it possible, by rational design of building blocks, to control

supramolecular architectures from spherical micelles, cylindrical micelles, vesicles, and toroids to nanotubes.^[5] Inspired by this elaboration, we envisioned that the control of the size and shape of artificial viruses would be possible if the preorganized supramolecular architectures used were robust polycationic scaffolds that remain unchanged after the formation of an interpolyelectrolyte complex (IPC) with negatively charged nucleic acids. Herein, we report a potentially generalizable strategy to create an artificial virus that memorizes the size and shape of its precursor. By using a preorganized supramolecular nanostructure as a template, we show that well-defined, discrete artificial viruses can be elaborated after IPC formation between the nanostructure and nucleic acids. This controlled feature and appropriate surface functionalization with multivalent carbohydrate ligands make the artificial virus highly efficient in the intracellular delivery of genes and drugs.

With the aim of constructing filament-shaped, discrete artificial viruses, a β -sheet peptide-based supramolecular building block (Glu-KW) was designed (Figure 1a). To our knowledge the filament-shaped artificial virus is unprecedented. It has been shown that the combination of hydrophobic and electrostatic interactions produced by the alternating placement of hydrophobic and charged amino acids in β -sheet peptides promotes β -sheet interaction and subsequent self-assembly into bilayered filamentous nanostructures (β ribbon).^[6] Coupling of hydrophilic segments, such as polyethylene glycol, hydrophilic peptides, or carbohydrates, to β -sheet peptides has been reported to stabilize β -ribbon nanostructures by suppressing lateral aggregate formation.^[6c-f]


The Glu-KW structure is characterized by a β -sheet-forming self-assembly segment, two linker segments, a nucleic acid-binding cationic segment, and a carbohydrate ligand segment. The β -sheet peptide segment consists of tryptophan–lysine–tryptophan–aspartic acid repeats, the amino acid configuration of which promotes β -sheet formation. The linker segments are designed to be flexible and nonionic by using glycine and serine residues. The eight lysine residues are placed between two linker segments to shield the cationic segment, upon self-assembly, from the β -ribbon surface. D-Glucose is positioned at the outermost part of Glu-KW to render the β -ribbon surface charge-neutral and to increase the chances of β -ribbon binding to the cell surface through multivalent interactions^[7] with cell-surface glucose transporters (GLUTs). GLUTs are present in nearly all mammalian cells and overexpressed in most cancer cells.^[8]

To address the question of whether Glu-KW forms β -sheet-mediated nanostructures, the self-assembly of Glu-KW was investigated by circular dichroism (CD) and transmission

[*] Dr. Y.-b. Lim, E. Lee, Y.-R. Yoon, Prof. M. Lee
Center for Supramolecular Nano-Assembly and
Department of Chemistry
Yonsei University, Seoul 120-749 (Korea)
Fax: (+82) 2-393-6096
E-mail: mslee@yonsei.ac.kr
Homepage: <http://csna.yonsei.ac.kr>

Dr. M. S. Lee
Department of Biochemistry, Yonsei University (Korea)

[**] We gratefully acknowledge the National Creative Research Initiative Program of the Korean Ministry of Science and Technology for financial support of this work.

 Supporting information for this article is available on the WWW under <http://www.angewandte.org> or from the author.

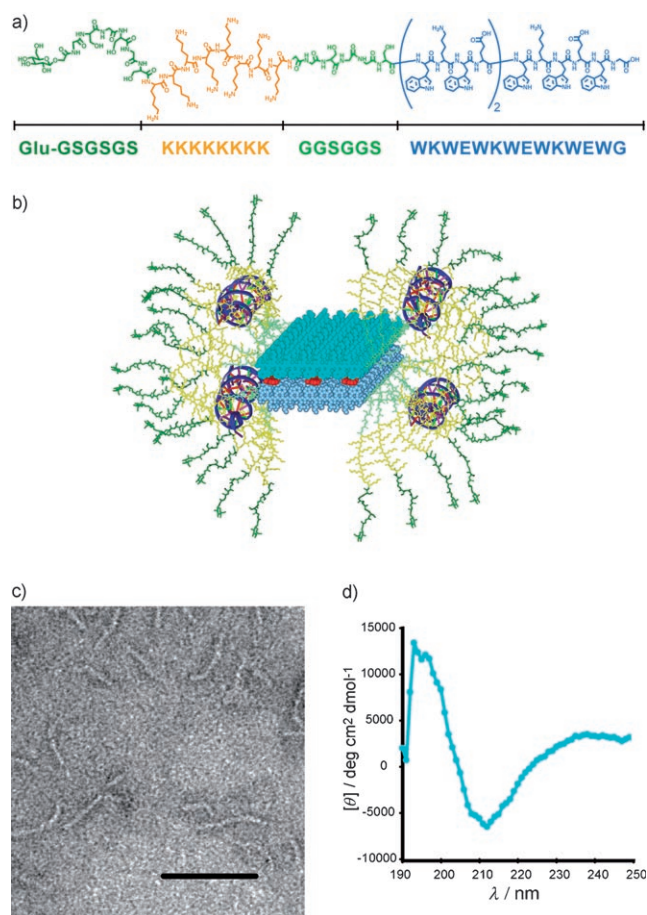


Figure 1. a) Structure of Glu-KW. A β -sheet peptide segment, nonionic segments (linkers and D-glucose), and a cationic segment are shown in blue, green, and yellow, respectively. Glu: D-glucose. For structures of all the building blocks (Glu-KW, NH₂-KW, FAM-KW, Man-RKW, and Glu-RKW; FAM = carboxyfluorescein, Man = mannose), see the Supporting Information. b) Molecular model of the artificial virus incorporating small interfering RNAs (siRNAs; blue, double-helix shape) and hydrophobic guest molecules (red). c) TEM image of a Glu-KW β ribbon. Scale bar: 100 nm. d) CD spectrum of Glu-KW (15 μM in PBS).

electron microscopy (TEM). The studies were performed in phosphate-buffered saline (PBS), a physiological buffer. The negative minimum of molar ellipticity at 213 nm in the CD spectrum indicates β -sheet interaction (Figure 1d). Indeed, the β -sheet interaction promoted the formation of discrete β ribbons, as revealed by TEM investigation (Figure 1c). The typical length of the β ribbon was relatively short at about 70 nm, which is likely to be advantageous for intracellular delivery applications.

We next asked whether the β ribbon can make IPCs with negatively charged small interfering RNA (siRNA) through the positively charged regions of the lysine residues. The siRNA is double-stranded RNA that is 21–23 nucleotides in length and induces sequence-specific post-transcriptional gene silencing called RNA interference (RNAi).^[10] RNAi is a powerful gene silencing process that holds great promise in the field of gene therapy.^[11] The siRNA gradually lost its electrophoretic mobility as the relative amount of the

β ribbon increased, thus indicating that β ribbon/siRNA complexes were formed (Figure 2a). The charge neutralization of the siRNA was achieved at a charge ratio (+/–) of

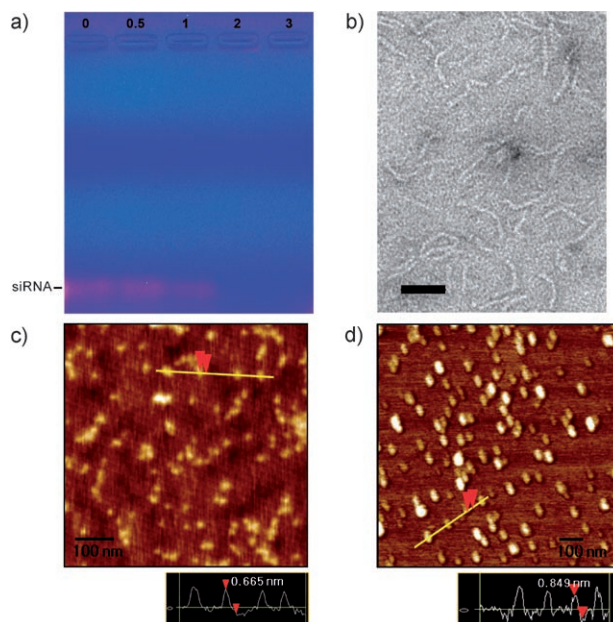


Figure 2. Formation of the artificial virus (β ribbon/siRNA complex). a) Change in electrophoretic mobility (4% agarose gel) of green fluorescent protein (GFP) siRNA after the addition of increasing amounts of Glu-KW β ribbon. The numbers indicate the charge ratio (+/–). b) TEM image of Glu-KW β ribbon/GFP siRNA complexes; +/–: 2. Scale bar: 50 nm. c, d) AFM images of Glu-KW β ribbons (c) and Glu-KW β ribbon/GFP siRNA complexes (d); +/–: 2.^[9] Diagrams beneath the images are height profiles along the yellow lines.

around 2. Remarkably, the TEM image of the β ribbon/siRNA complexes showed that the β ribbon maintained its discrete and short nanoribbon morphology even after siRNA complexation (Figure 2b). Atomic force microscopy (AFM) investigation revealed that the height of the β ribbon grew from 0.67 to 0.85 nm after siRNA addition, which indicates that β ribbon/siRNA complexes were formed (Figure 2c,d).^[9]

Upon mixing the Glu-KW β ribbon with siRNA, the positive CD band of the siRNA at 261 nm increased and underwent a long-wavelength shift of 19 nm (see the Supporting Information). These CD changes are characteristic of double-stranded RNA in a condensed state,^[12] and indicate that the siRNA binds directly to the cationic segment of the Glu-KW β ribbon. In addition, a CD experiment with double-stranded DNA (dsDNA) of the same size as the siRNA showed that the intensity of the negative CD band of the dsDNA at 250 nm increased and the positive CD band at 279 nm underwent a long-wavelength shift (see the Supporting Information). These CD changes represent the characteristic transition of the DNA structure from the B type to the Ψ -DNA type.^[13] The formation of Ψ -DNA is an indication of dehydration and neutralization of DNA phosphate groups by polycations. The evidence clearly indicates that the nucleic

acids (siRNA and dsDNA) interact directly and strongly with the cationic segment of the Glu-KW β ribbon.

The hydrodynamic radius (R_H) of the β ribbon remained unchanged after complex formation. In stark contrast, the R_H of a β ribbon self-assembled from a building block devoid of glucose (NH₂-KW) increased abruptly following siRNA complexation (see the Supporting Information). Inter-ribbon cross-linking induced by the addition of negatively charged siRNA should be responsible for this phenomenon, as the surface of the NH₂-KW β ribbon is densely coated with positively charged primary amine groups.

All these results indicate, as the molecular model in Figure 1b suggests, that the capacity of positively charged regions created by β -ribbon formation is large enough to incorporate relatively small interfering RNA inside, and that the glucose-covered charge-neutral surface is crucial in preventing uncontrollable aggregation of the elementary β ribbons. The other building blocks (Man-RKW and Glu-RKW) designed through the same concept as the Glu-KW showed a similar siRNA complexation behavior, thus indicating that the strategy is potentially generalizable (see the Supporting Information).

To address the potential of the Glu-KW artificial virus as an intracellular siRNA delivery carrier, an RNAi experiment with GFP was conducted on HeLa cells, a human cervical cancer cell line. As shown in Figure 3a, GFP knockdown

experiments performed in the absence of serum showed that the Glu-KW β ribbon was even better than Lipofectamine 2000 (LF2000), a commercial reagent known to have one of the highest siRNA transfection efficiencies. This promising result led us to investigate the gene knockdown efficiency in the presence of serum, a condition representing an in vivo physiological milieu. The results showed that the efficiency of GFP knockdown by the Glu-KW β ribbon is comparable to that of LF2000 (Figure 3b). LF2000 is known to have high siRNA transfection efficiency in the presence of serum as well. In contrast, the NH₂-KW β ribbon was almost unable to transfect siRNA. Hence, the discrete nanostructures encapsulating siRNA within the noncharged surface are crucial for the high transfection efficiency. Several important factors are likely to be synergistically involved in the high siRNA transfection efficiency of the Glu-KW artificial virus, such as controlled formation of artificial viruses, minimal interaction with serum proteins by the charge-neutral surface, and enhancement of the cell interaction by multivalent coating of carbohydrate ligands.

As the interfacial hydrophobic space formed within the bilayered β ribbon is a suitable place to encapsulate hydrophobic guest molecules,^[6d] we next addressed the question of whether the β ribbon can deliver siRNA while encapsulating such guest molecules. For this we first encapsulated a hydrophobic guest (nile red) within a Glu-KW β ribbon and then siRNA was complexed with the Glu-KW β ribbon/nile red binary complex. The ternary complex was still able to knock down GFP expression, albeit the efficiency was slightly decreased compared to that of a Glu-KW β ribbon without Nile red (Figure 3b). Nile red delivered by the ternary complex was localized not only in the cytoplasmic compartment but also in the nucleus (Figure 3c). The nucleus is the site of action for many drugs and most anticancer drugs. Therefore, the Glu-KW artificial virus has the potential to become an efficient nanomaterial for delivering a hydrophobic drug and gene simultaneously into the cell nucleus as well as the cytoplasm.

To gain further insight into the intracellular distribution and delivery mechanism, Glu-KW was co-assembled^[6d] with a fluorescently labeled building block (FAM-KW) to label the β ribbon. The image in Figure 3d shows the intracellular pattern of β -ribbon distribution (green), which suggests an endocytic entry pathway^[14]. In addition, co-localization (yellow) of the β ribbon and LysoTracker (red) further demonstrates an endocytotic uptake mechanism. LysoTracker is an acidotropic reagent for labeling and tracing acidic organelles, such as late endosomes and lysosomes, in live cells.

In summary, we have demonstrated that directed assembly of an artificial virus is possible by using rationally designed, preorganized β ribbons. A unique feature of our nanostructure is its capability to encapsulate siRNA within the noncharged carbohydrate surfaces while preserving its discrete nanostructure. Considering the variety of supramolecular nanostructures that are currently or will be available, this type of approach provides a general means to construct various repertoires of controllable artificial viruses. It is anticipated that other functional properties of natural viruses could be further finely installed in this artificial virus,

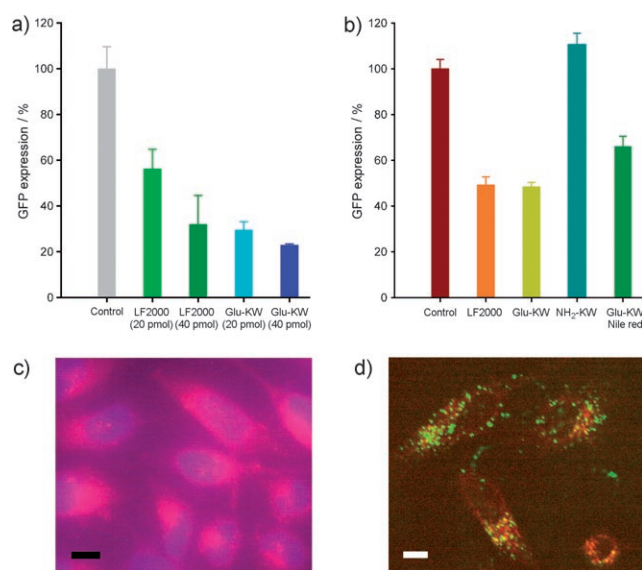


Figure 3. Intracellular deliveries of siRNA and hydrophobic guest molecules. a) Knockdown of GFP expression in HeLa cells. The numbers in parentheses indicate the amounts of GFP siRNA used. The experiment was performed in the absence of serum (mean \pm standard deviation (SD), $n = 3$). b) Knockdown experiment performed with 40 pmol GFP siRNA in the presence of 10% serum (mean \pm SD, $n = 3$). c) Intracellular distribution of Nile red (red) delivered by the ternary complex of Glu-KW, Nile red, and GFP siRNA. The nucleus was stained with 4'-6-diamidino-2-phenylindole (blue). Scale bar: 50 μ m. d) Intracellular distribution studies by confocal laser scanning microscopy. The Glu-KW/FAM-KW β ribbon and LysoTracker Red DND-99 are shown in green and red, respectively. Glu-KW and FAM-KW were co-assembled at 100:1 molar ratio. Scale bar: 50 μ m.

which will ultimately lead to the generation of safe and efficient artificial viruses for gene and drug delivery.

Received: January 18, 2008
Published online: May 7, 2008

Keywords: drug delivery · nanomaterials · peptides · supramolecular chemistry · viruses

- [1] a) E. Mastrobattista, M. A. E. M. van der Aa, W. E. Hennink, D. J. A. Crommelin, *Nat. Rev. Drug Discovery* **2006**, *5*, 115–121; b) D. W. Pack, A. S. Hoffman, S. Pun, P. S. Stayton, *Nat. Rev. Drug Discovery* **2005**, *4*, 581–593; c) N. Nishiyama, A. Iriyama, W.-D. Jang, K. Miyata, K. Itaka, Y. Inoue, H. Takahashi, Y. Yanagi, Y. Tamaki, H. Koyama, K. Kataoka, *Nat. Mater.* **2005**, *4*, 934–941; d) K. C. Wood, S. R. Little, R. Langer, P. T. Hammond, *Angew. Chem.* **2005**, *117*, 6862–6866; *Angew. Chem. Int. Ed.* **2005**, *44*, 6704–6708; e) G. Zuber, L. Zammuto-Italiano, E. Dauty, J.-P. Behr, *Angew. Chem.* **2003**, *115*, 2770–2773; *Angew. Chem. Int. Ed.* **2003**, *42*, 2666–2669; f) D. De Paula, M. V. L. B. Bentley, R. I. Mahato, *RNA* **2007**, *13*, 431–456; g) Y.-b. Lim, C.-h. Kim, K. Kim, S. W. Kim, J.-s. Park, *J. Am. Chem. Soc.* **2000**, *122*, 6524–6525.
- [2] A. V. Kabanov, F. C. Szoka, Jr., L. W. Seymour in *Self-Assembling Complexes for Gene Delivery: From Laboratory to Clinical Trial* (Eds.: A. V. Kabanov, P. L. Felgner, L. W. Seymour), Wiley, New York, **1998**, pp. 197–218.
- [3] Y. Aoyama, T. Kanamori, T. Nakai, T. Sasaki, S. Horiuchi, S. Sando, T. Niidome, *J. Am. Chem. Soc.* **2003**, *125*, 3455–3457.
- [4] Y. Geng, P. Dalhaimer, S. Cai, R. Tsai, M. Tewari, T. Minko, D. E. Discher, *Nat. Nanotechnol.* **2007**, *2*, 249–255.
- [5] a) J.-M. Lehn, *Proc. Natl. Acad. Sci. USA* **2002**, *99*, 4763–4768; b) T. Shimizu, M. Masuda, H. Minamikawa, *Chem. Rev.* **2005**, *105*, 1401–1443; c) M. Lee, B.-K. Cho, W.-C. Zin, *Chem. Rev.* **2001**, *101*, 3869–3892; d) I. W. Hamley, V. Castelletto, *Angew. Chem.* **2007**, *119*, 4524–4538; *Angew. Chem. Int. Ed.* **2007**, *46*, 4442–4455; e) S. Zhang, *Nat. Biotechnol.* **2003**, *21*, 1171–1178; f) D. J. Pochan, Z. Chen, H. Cui, K. Hales, K. Qi, K. L. Wooley, *Science* **2004**, *306*, 94–97.
- [6] a) D. M. Marini, W. Hwang, D. A. Lauffenburger, S. Zhang, R. D. Kamm, *Nano Lett.* **2002**, *2*, 295–299; b) C. W. G. Fishwick, A. J. Beevers, L. M. Carrick, C. D. Whitehouse, A. Aggeli, N. Boden, *Nano Lett.* **2003**, *3*, 1475–1479; c) D. Eckhardt, M. Groenewolt, E. Krause, H. G. Börner, *Chem. Commun.* **2005**, 2814–2816; d) Y.-b. Lim, E. Lee, M. Lee, *Angew. Chem.* **2007**, *119*, 3545–3548; *Angew. Chem. Int. Ed.* **2007**, *46*, 3475–3478; e) Y.-b. Lim, S. Park, E. Lee, H. Jeong, J.-H. Ryu, M. S. Lee, M. Lee, *Biomacromolecules* **2007**, *8*, 1404–1408; f) Y.-b. Lim, S. Park, E. Lee, J.-H. Ryu, Y.-R. Yoon, T.-H. Kim, M. Lee, *Chem. Asian J.* **2007**, *2*, 1363–1369.
- [7] a) M. Mammen, S.-K. Choi, G. M. Whitesides, *Angew. Chem.* **1998**, *110*, 2908–2953; *Angew. Chem. Int. Ed.* **1998**, *37*, 2754–2794; b) Y.-b. Lim, M. Lee, *Org. Biomol. Chem.* **2007**, *5*, 401–405.
- [8] M. L. Macheda, S. Rogers, J. D. Best, *J. Cell. Physiol.* **2005**, *202*, 654–662.
- [9] It was difficult to obtain a clear AFM image of Glu-KW β ribbons, probably because of the flexible properties of the hydrophilic segments. The width of the ribbons and complexes appears thicker than their actual size because of a tip-broadening effect. This effect makes the cylindrically shaped ribbons look like elongated spheroids.
- [10] A. Fire, S. Xu, M. K. Montgomery, S. A. Kostas, S. E. Driver, C. C. Mello, *Nature* **1998**, *391*, 806–811.
- [11] S. I. Pai, Y.-Y. Lin, B. Macaes, A. Meneshian, C.-F. Hung, T.-C. Wu, *Gene Ther.* **2006**, *13*, 464–477.
- [12] H. T. Steely, Jr., D. M. Gray, D. Lang, M. F. Maestre, *Biopolymers* **1986**, *25*, 91–117.
- [13] C. Arigita, N. J. Zuidam, D. J. A. Crommelin, W. E. Hennink, *Pharm. Res.* **1999**, *16*, 1534–1541.
- [14] S. Veldhoen, S. D. Laufer, A. Trampe, T. Restle, *Nucleic Acids Res.* **2006**, *34*, 6561–6573.